Journal of Biomechanics 46 (2013) 964–972

Contents lists available at SciVerse ScienceDirect

Journal of Biomechanics

journal homepage: www.elsevier.com/locate/jbiomech
www.JBiomech.com

The effects of damage accumulation on the tensile strength and toughness of compact bovine bone

Wei Zhang [a], Srinivasan Arjun Tekalur [a,*], Melissa Baumann [b], Laura R. McCabe [c]

[a] Department of Mechanical Engineering, Michigan State University, East Lansing, MI 48824, United States
[b] Department of Chemical Engineering and Materials Science, Michigan State University, East Lansing, MI 48824, United States
[c] Departments of Physiology and Radiology, Michigan State University, East Lansing, MI 48824, United States

ARTICLE INFO

Article history:
Accepted 6 December 2012

Keywords:
Bone
Tensile failure
Microcracking
Damage
Strain rate
Osteon

ABSTRACT

Damage accumulation in compact bovine femur subjected to uniaxial tensile loading was examined by strong light illumination effects of microcracking. Imaging was done using a high-speed camera capturing image at 200 to 1500 FPS. The tensile tests were performed in a multipurpose tensile testing system with cross-head speeds ranging from 0.5 to 10 mm/min which leads to strain rates of 0.0001 to 0.0012 s^{-1} (physiologically relevant to walking and running Hansen et al., 2008). The post-failure images were then examined in a scanning electron microscopy (SEM) and effects of microstructure, strain rate, and orientation were evaluated. Correlation of the high-speed images with stress–strain curves indicated that optically visible microcracks were most likely initiated at yielding, and the specimens with dispersed microcracks exhibited a higher energy-absorption capacity compared to the specimens with coalesced local cracks. It was found that damage accumulation negatively correlates to strain rate and that transverse specimens exhibited a different failure pattern compared to the longitudinal specimens. Strain hardening and softening were found in the longitudinal and transverse specimens respectively. The microcracking in the transverse specimens instantly increased to peak after yielding compared to the gradual growth until failure in the longitudinal specimens. The average Young's modulus (21.5 GPa) and ultimate stress (93.5 MPa) of the specimens loaded in the longitudinal direction were more than twice that of the specimens (10.9 GPa and 36.2 MPa respectively) loaded in the transverse direction. The current technique has shown potential in relating damage accumulation real time in bone samples subjected to tensile loading condition. This information will be helpful in relating the role of micro damage accumulation in initiating failure and/or remodeling in bone.

1. Introduction

As a tough and light-weight natural composite, bone provides support and protection to internal organs. Understanding the failure mechanisms in bone is of great medical interest for preventing bone fracture failure and improving bone fracture treatment. Adult cortical bone is weak in tension and shear and strong in compression (Carter et al., 1981; Crowninshield and Pope, 1974; Currey and Brear, 1974; Turner, 2006). Bone is a strain-rate-dependent material due to its viscoelastic properties where increases in loading rate have resulted in increases in Young's modulus and ultimate stress (Adharapurapu et al., 2006; Currey, 1975; Ferreira et al., 2006; Hansen et al., 2008; Mcelhane, 1966; Pithioux et al., 2004; Saha and Hayes, 1976). The mechanical properties of compact bone are also related to its hierarchical microstructure. The strength, energy absorption, and modulus of elasticity decrease with the percentage area of osteons (Mcelhane, 1966; Robertson and Smith, 1978; Saha and Hayes, 1976, 1977; Wright and Hayes, 1976). Interestingly, little emphasis has been placed on the role of microcracking on the tensile failure behavior of bone, although, like quasi-brittle materials, failure of bone is characterized as the result of damage accumulation in the form of microcracks.

Microcrack accumulation has been shown to produce a loss of stiffness in compact bone under cyclic fatigue testing (Burr et al., 1997; Reilly and Currey, 2000; Schaffler et al., 1990). Microcracking was also found to be a primary toughening mechanism that resulted in better *R*-curve behavior (Vashishth et al., 1997, 2000, 2003). O'Brien et al. (2003) applied a series of fluorescent chelating agents to monitor crack growth during cyclic compression fatigue finding that microcracking initiated in the interstitial bone tissue in the early stage of the fatigue life and that longer microcracks developed in the longitudinal direction as opposed to the transverse direction. In recent efforts, Zioupos et al. (2008)

* Correspondence to: Department of Mechanical Engineering, Michigan State University, 2727 Alliance Drive, Suite B, Lansing, MI 48910, United States. Tel.: +1 517 884 1608; fax: +1 517 884 1601.
E-mail address: tsarjun@egr.msu.edu (S.A. Tekalur).

0021-9290/$ - see front matter © 2012 Elsevier Ltd. All rights reserved.
http://dx.doi.org/10.1016/j.jbiomech.2012.12.005

examined the plastic strain of compact canine femurs, subjected to tensile loading at various strain rates, to the number of cracks (imaged by staining), concluding that the plastic strain had positive correlation with the number of cracks. However, each of the above studies were limited by the resolution limits imposed by Frost's (1960) bulk fuchsin staining technique which requires the tested specimens to be cut into microsections which compromise the accuracy of the crack length measurement. Several attempts have been made to avoid these limitations. Zioupos et al. (1994) used the acoustic emission method to monitor crack growth in bone and antler specimens under uniaxial tensile loading where microcracks were found to initiate upon yielding in both antler and bovine tibia specimens. However, the shortcoming of the technique is that the growth and distribution of microcracks cannot be directly visualized. Using the laser illumination technique, Reilly and Currey (1999) found that the microcracks developed on the tensile side of bone specimens subjected to four-point bending. These tensile microcracks first appeared at a strain of 0.004 and the peak growth of the microcracks occurred when the strain reached 0.008. However, due to the step loading and examination, the stress–strain curve was not continuously obtained throughout the test.

In the present paper, an innovative optical technique was used to monitor the damage accumulation during the process of tensile failure of compact bovine femur. A high speed camera and a LED panel were set up to record the light illumination of the microcracks initiated and propagating on the specimen surface when stretched in a multipurpose tensile testing system (MTS). By using strong light scattering effects of crack edges, microcracks were visible as features with higher light intensity (Fig. 2). The approach cannot quantify the exact amount of microcracking in bone but rather indirectly provides "real-time" relationship between microcracking and strain development while the bone is subjected to tensile loading. The images shown are real time images of micro crack development. The focus of the paper is on existence of critical strain rate, critical strain levels, and orientation effects for initiation and propagation of microcracking. To evaluate the correlation between the developing microcracks and the bone microstructure, specimens from bovine femurs (12–30 months old) were examined. Strain rate effects were also investigated by examining 10 specimens from one piece of bovine femur with strain rates ranging from 0.0001 to 0.0012 s^{-1}. As a natural composite material, the mechanical properties of bone depend on the fiber or osteon direction, which runs along the loading axis of bone (Rho et al., 1998). It has been shown that osteons potentially act as barriers to prevent coalescence of the microcracks initiated in the interstitial bone tissue (Nalla et al., 2004, 2005). Thus, the failure pattern of bone loaded in the transverse (perpendicular to the osteon direction) and the longitudinal direction (along the osteon direction) are expected to be different. To evaluate such orientation effects, the compact bovine specimens machined from one piece of bovine femur bone were loaded in the longitudinal and transverse directions. The stress–strain curves were correlated with the high-speed images to examine the microcrack growth in the specimens. Post-failure examinations were performed with a scanning electron microscope (SEM). Both the front flat surface (the surface facing the camera) and the fracture surface were examined.

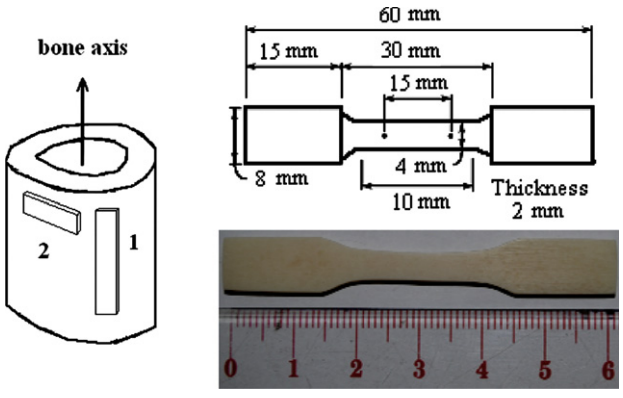

Fig. 1. Geometry and dimensions of dog-bone specimens. (a), specimen orientation diagram (1), longitudinal specimens, loaded along the osteon direction; (2, transverse specimens, loaded perpendicular to the osteon direction); (b), the dimension of the longitudinal specimens (the length of the transverse specimens is half of the longitudinal specimens).

2. Material and methods

The tensile specimens were machined from fresh compact femurs of skeletally mature bovines (12 to 30 months old) provided by a local beef abattoir. The mid-diaphysis of the bovine femur was first cut into rough rectangular beams using a band saw. Then, the beams were machined into $60 \times 8 \times 2$ mm^3 (longitudinal) or $30 \times 8 \times 2$ mm^3 (transverse) rectangular shapes using a milling machine (ProCut RL80RF311) at a low feed speed. Subsequently, a Dremel hand tool was used to shape the rectangular beams into the dog-bone shape specimens with exactly the same geometry. Finally, the specimens were manually polished by 80, 100, 600 and 1000 grit. During the entire machining process, the specimens were kept wet with phosphate buffered saline (PBS) solution. The geometry and dimensions are shown in Fig. 1. After machining, the specimens were covered with gauge dipped in PBS solution and preserved in a -20 °C freezer until testing. Specimens were thawed prior to testing. Overall, 28 specimens were machined, including 12 specimens from one femur (30-months old) for strain rate effects, 10 specimens from several femurs with various ages (12 to 30 months old) for microstructure effects, and 6 specimens from one femur (30-months old) to examine orientation effects.

Uniaxial tensile testing was performed using a MTS Insight tensile testing system with a 10 kN load cell. A high speed camera (Phantom V12) was set facing the front side of the specimen to record the fracture process. In order to visualize the microcracks, the tests were performed in a dark room and a strong cold light source was set at the side of the camera to illuminate the specimen. A laser extensometer (EIR Model LE-05) was set up facing the back side of the specimen to measure the extension. Both the high speed camera and the laser extensometer were triggered at the same time as the MTS started to apply the load. The rationale of the research approach is not directed to quantify the exact amount of microcracking in bone but rather indirectly provide "real-time" relationship between microcracking and strain development. It is proposed that there exist critical strain rate and strain levels to initiate and propagate microcracking in bone. It has never been clearly shown what these levels are. More importantly, orientation of bone and the osteon size affects initiation and propagation of microcracking. The experimental design is geared to bring out these effects. Since we indirectly correlated microcracking by the diffuse light pattern, questions might arise on validity of using the light intensity as a measure of microcracking. It is true that many materials exhibit change in color or appearance while subjected to loading (e.g. crazing in polymers). But it is different in case of bone where the change in light intensity is directly related to microcracking. Validation for the current is provided by Zioupos et al. (2008) and in our experimental measurements themselves where the light diffusion gradually increases as the load is applied and reaches peak value at peak load (Fig. 2). Exact quantification of light intensity to density of microcracking could be undertaken but again is not the primary focus of the current work

The specimens were covered with sterile PBS soaked gauze before testing, where the duration of the test lasted about one minute. Thus, the specimens were considered wet. For the strain rate evaluation, the cross-head speeds ranged from 0.5 mm/min to 10 mm/min corresponding to strain rates of 0.0001 to 0.0012 s^{-1}. All other tests were performed at a cross-head speed of 0.5 mm/min. The frame rates of the high speed camera were 200 s^{-1}, 800 s^{-1}, and 1500 s^{-1} for tests with cross-head speeds of 0.5 mm/min, 1 to 2 mm/min, and larger than 3 mm/min, respectively. Images from the camera were used to calculate the light intensity in each frame by a MATLAB code. The light intensity was represented the normalized gray scale value in each frame, which was calculated by summarizing the gray scale value of each pixel in each frame after subtracting the corresponding value in the reference frame (the frame at the onset of loading), and then normalizing by the numbers of pixel in the frame.

The post-failure fracture damage of the tested specimens was examined in a JEOL JSM-6400V (lanthanum hexaboride electron emitter) scanning electron microscope. Digital images were acquired using analySIS Pro software version 3.2 (Olympus Soft Imaging Solution Corp., Münster, Germany). Before the examination, samples were coated with gold (≈ 20 nm thickness) in an Emscope